



ELSEVIER

SCIENCE @ DIRECT®

MICROELECTRONIC  
ENGINEERING

Microelectronic Engineering 67–68 (2003) 609–614

[www.elsevier.com/locate/mee](http://www.elsevier.com/locate/mee)

# Fabrication and application of a full wafer size micro/nanostencil for multiple length-scale surface patterning

G.M. Kim<sup>1</sup>, M.A.F. van den Boogaart, J. Brugger\**Microsystems Laboratory, Institute of Microelectronics and Microsystems, Swiss Federal Institute of Technology (EPFL), 1015 Lausanne, Switzerland*

---

## Abstract

A tool and method for flexible and rapid surface patterning technique beyond lithography based on high-resolution shadow mask method, or nanostencil, is presented. This new type of miniaturized shadow mask is fabricated by a combination of MEMS processes and focused ion beam (FIB) milling. Thereby apertures in a 100–500 nm thick low-stress silicon nitride membrane in the size range from  $< 100$  nm to  $> 100$   $\mu\text{m}$  were made. The stencil device is mechanically fixed on the surface and used as miniature shadow mask during deposition of metal layers. Using this method, aluminum micro- and nanostructures as small as 100 nm in width were patterned. The deposited micro- and nano-scale structures were used as etch mask and transferred into a sub-layer (in our case silicon nitride) by dry plasma etching. High-resolution shadow masking can be used to create micro/nanoscale patterns on arbitrary substrates including mechanically fragile or chemically active surfaces.

© 2003 Elsevier Science B.V. All rights reserved.

*Keywords:* Nanostencil; Shadow mask deposition; Nanoengineering; Focused ion beam milling; MEMS technology

---

## 1. Introduction

Sub-micron scale lithography methods using deep UV, X-ray or electron beams allow further progress to be made in the field of highly integrated circuit hardware manufacturing. One drawback of high-end patterning methods, however, is firstly, the high cost of the equipment. Secondly, a major technical limitation of resist-based lithography is that it cannot be applied to mechanically unstable and bio/chemically functional surface layers. With the advent of nano/micro-electro-mechanical systems (NEMS/MEMS) having higher complexity and integrated functionality, polymer-based

---

\*Corresponding author.

*E-mail address:* [Juergen.brugger@epfl.ch](mailto:Juergen.brugger@epfl.ch) (J. Brugger).

<sup>1</sup>Present address: School of Mechanical Engineering, Kyungpook National University, 702-701 Daegu, South Korea.

electronic devices, microfluidics, and bio-analytical systems, increased flexibility of the surface patterning methods becomes important. Emerging micro- and nanopatterning methods such as the local deposition of molecular layers by micro-contact printing ( $\mu$ CP) [1,2], thermo-mechanical indentation of polymers by nanoimprint lithography (NIL) [3] or surface modification by scanning probe lithography (SPL) [4] are opening new possibilities to address these issues, by providing improved flexibility and increased functionality potentially at low cost. Another interesting patterning method is based on the local material deposition through miniature shadow-masks. This resistless and virtually contact-free method totally avoids the risk of chemical cross-contamination and/or mechanical substrate damage. In the past, the technique has been applied on the micrometer scale using microfabricated solid-state [5–7], casted elastomeric [8] and photoplastic [9] membranes. In order to reach the sub-micron scale pattern, the membranes need to be thinned further down. Recently, ultra-thin (50–300 nm thick) solid-state silicon nitride (SiN) membranes have been used as shadow-mask for the patterning of 10–300-nm scale structures [10,11]. However, due to the low mechanical stability of such freestanding membranes to sustain the stress induced by the deposited layer the membrane area was limited within an area of a few tens of  $\mu\text{m}^2$ . In order to advance this promising method further, we have investigated in the micro/nanoengineering of a new type of free-standing SiN membranes with the objective to enable shadow-mask techniques that can be applied simultaneously to both, the micrometer and nanometer scale on a full-wafer scale (100 mm). Such a MEMS based nanostencil allows high-throughput, large area nanopatterning beyond resist based lithography.

## 2. Nanostencil fabrication process

Fig. 1 shows schematic diagrams of the MEMS and nano-engineered shadow mask and the local deposition method. The shadow mask has both  $\mu\text{m}$ - and nano-scale apertures in the same membrane in close proximity, which will allow micro- and nanoscale features to be connected together. The  $\mu\text{m}$ -scale apertures were defined by standard optical photolithography process and dry etching into a 500-nm thick silicon nitride (SiN). The  $2 \times 2$ -mm large membranes were released by isotropic wet etching of silicon (Si) substrate from backside.

Fig. 2 shows the schematic overview of the nanostencil fabrication process. The process starts with

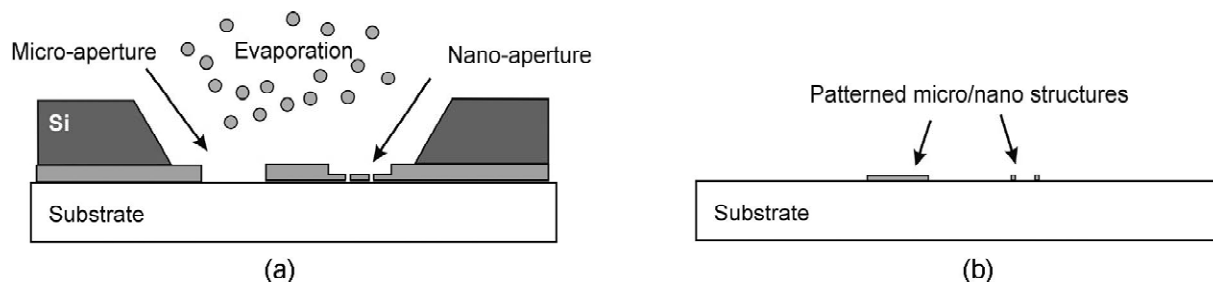


Fig. 1. (a) Schematic diagram of shadow mask with two-level thickness: 500-nm thick membrane for the micro apertures and 50-nm thick membrane for the nano-structures. The material is locally deposited onto the substrate through the apertures in the shadow mask. (b) After the shadow mask is removed, the micro-/nano-structures are a 1:1 copy of the aperture patterns in the shadow mask membrane.

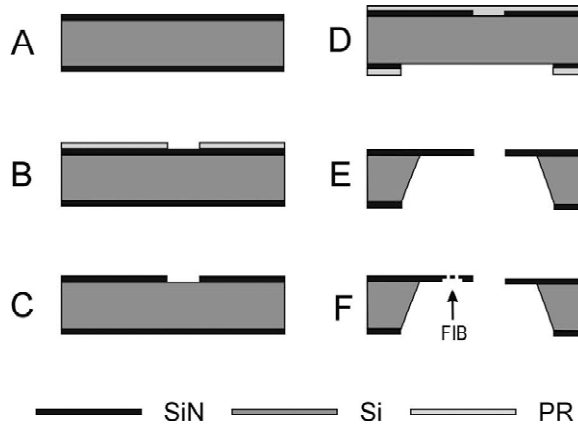


Fig. 2. Schematic overview of nanostencil fabrication process. (a) Deposition of 500-nm thick low stress SiN. (b) Photolithography of microscale pattern. (c) SiN etching of microscale pattern. (d) Photolithography and SiN etching on backside. (e) KOH etching of bulk Si from backside for 500-nm thick SiN membrane releasing. (f) FIB milling for local SiN membrane thinning into 50-nm thick, and then, nanoaperture fabrication.

the deposition of 500-nm thick low-stressed SiN by low-pressure chemical vapour deposition (LPCVD) on a double-side polished, 380- $\mu\text{m}$  thick silicon wafer. The internal tensile stress of the SiN layer is about 200 MPa. Micro-scale patterns were defined in 1.7- $\mu\text{m}$  thick positive photoresist (S1818, Shipley) on topside by means of conventional photolithography (MA-150 aligner, Karl Süss). The micro-scale resist patterns were transferred into the SiN layer by subsequent anisotropic etching using inductively coupled plasma (ICP) (601E, Alcatel:  $\text{C}_2\text{F}_6$  20 sccm, 20 °C, 1800 W). In the same way, the backside patterns were etched into backside SiN layer to be used as etch mask during the backside etching of the silicon substrate in order to release the SiN membrane. Potassium hydroxide (KOH) was used (40 wt%, 60 °C) for the bulk etching of the Si and to release the membrane. Fig. 3

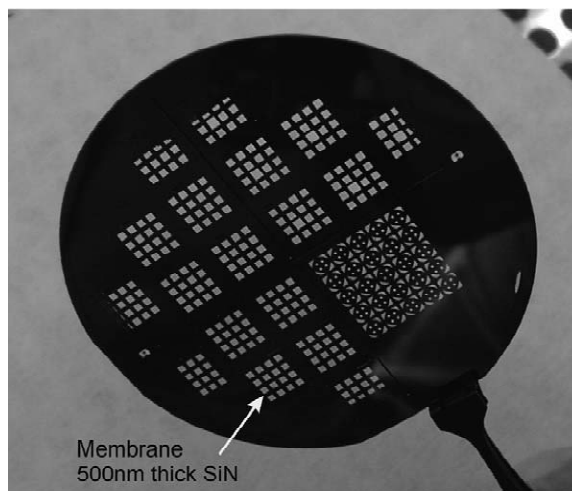


Fig. 3. Photograph of a 100-mm wafer shadow mask containing 388 membranes fabricated by MEMS process.

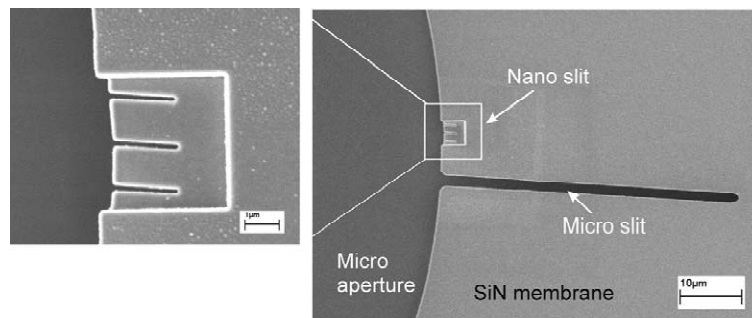


Fig. 4. Scanning electron microscopy (SEM) images of multiple-length scale apertures in a shadow mask. Right: micro- and nano-apertures made in single membrane. The micro slit aperture is 1.5- $\mu\text{m}$  wide and 50- $\mu\text{m}$  long. Left: an enlarged view of the nano-apertures. The dimension of the nano slit aperture is 170-nm wide and 2- $\mu\text{m}$  long. Both of the images were taken after evaporation of 100-nm thick aluminium.

shows an optical photograph of a finished microfabricated 100-mm full wafer that contains 388 membranes with various aperture patterns in the micro-scale.

As our conventional optical lithography (mask writer and aligner) is limited to about 1  $\mu\text{m}$  resolution we used a focused ion beam (FIB) milling to define sub-micron structures in the suspended membrane. As the size of the aperture is getting smaller, the aspect ratio of the membrane thickness to the aperture size becomes larger. For example, the aspect ratio of a 100-nm aperture to a 500-nm thick membrane is 5, which makes it difficult for material to pass through the aperture due to the shadow effect of the aperture sidewall itself. On the other hand, a thinner membrane is mechanically less stable. For this reason, we have locally thinned down the membrane at the location of the nano-scale apertures prior to the drilling of the apertures themselves. In order to stabilize the ion beam during the FIB process, a 5-nm thick gold layer was deposited onto the dielectric SiN layer. Firstly, the 500-nm thick membrane near apertures was locally thinned down to 50-nm thick ( $2.0 \text{ nC}/\mu\text{m}^2$  at 0.2 nA), and then the nano-scale apertures were drilled ( $0.1 \text{ nC}/\mu\text{m}^2$  at 0.2 pA). Fig. 4 shows scanning electron microscopy (SEM) images of  $\mu\text{m}$ - and nano-scale apertures made in a SiN membrane. The right figure shows micro- and nano-apertures in close proximity to each other. The left figure is an enlarged image of the nano-apertures. The micro-slit is 1.5  $\mu\text{m}$  wide and 50  $\mu\text{m}$  long. The nano-slit apertures are 170 nm wide and 2  $\mu\text{m}$  long.

### 3. Rapid and simultaneous micro- and nanoscale patterning

We performed deposition through the fabricated shadow mask. The shadow mask was mechanically fixed on the substrate during the deposition. Before deposition, the shadow mask was inspected using SEM to check if the shadow mask and substrate were in contact. A 100-nm thick aluminium (Al) layer was locally deposited through shadow mask on full wafer scale. The deposition was done on a 200-nm thin silicon nitride layer, which was previously deposited on the silicon substrate. E-beam evaporation was used for the Al deposition (EVA-600, Alcatel, base chamber pressure  $5 \times 10^{-7}$  mbar). After removing the stencil from the surface, Al nanostructures as small as  $\sim 100$  nm were successfully patterned through the fabricated shadow mask as shown in Fig. 5. Fig. 5a shows a SEM

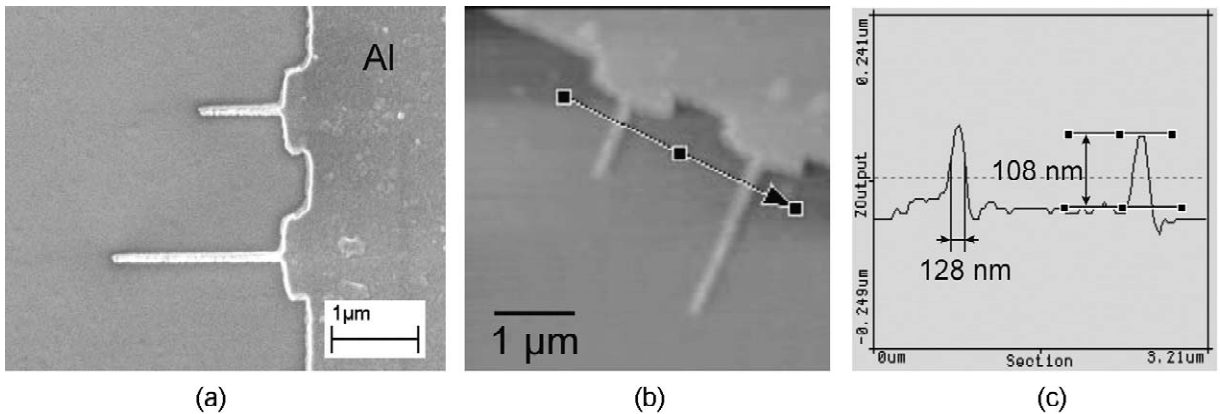


Fig. 5. SEM image and AFM image of Al nanostructures evaporated through shadow mask. (a) SEM image, (b) AFM image, and (c) topography of the nanostructures. The measured thickness of Al layer was about 100 nm. The measured width (FWHM) of a nanostructure was 128 nm.

image of metal nanowires ( $\sim 100$  nm wide, 1 and 2  $\mu\text{m}$  long) made by means of shadow evaporation through the micro/nanostencil. AFM analysis of the evaporated patterns is shown in Fig. 5b and c. In this case, the AFM measured thickness of the Al layer is 108 nm and the measured width is 128 nm. One of the advantages of this method is that a stencil can be used many times. During the deposition, the material covers the membrane as well as the target surface making it necessary to clean the membrane after certain times of usage. The gradual clogging of the aperture in the membrane accompanying the evaporation can be reduced by coating a self-assembled monolayer on the membrane surface [12].

The evaporated metal layer can be used directly as structural layer, e.g. micro- and nanoelectrodes, or, it can also be used as etch mask for a subsequent pattern transfer process. Fig. 6a shows an example of such a process, where 100-nm thick Al micro- and nanopatterns are used as mask for further etching of 200-nm thick silicon nitride (601E, Alcatel:  $\text{C}_2\text{F}_6$  20 sccm, 20 °C, 1800 W). The

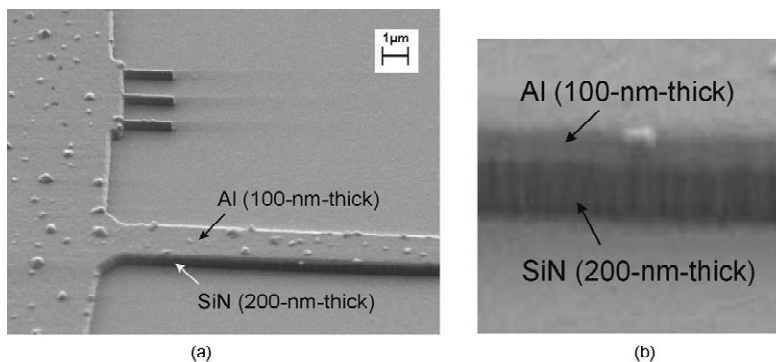


Fig. 6. SEM images of (a) the bi-layer micro-/nano-structure of the SiN and Al layer. The 100-nm thick Al layer was evaporated through the shadow mask. The deposited micro- and nano-scale structures have been transferred into SiN using Al layer as etch mask. (b) The interface of Al and SiN is clearly visible.

interface of Al and SiN is clearly visible in Fig. 6b. These results show that shadow mask patterning can be applied as rapid patterning method on multiple length scales from 100-nm to several 100  $\mu\text{m}$ .

#### 4. Conclusions

A new type of miniature micro/nanostencil is presented that can be used as shadow mask tool for simultaneous, high-throughput, micro- and nanoscale patterning on large surface area, at potentially low-cost, which is a difficult task for standard lithography techniques. The full wafer scale SiN membrane nanostencils (shadow masks) include multiple length scale apertures ranging from 100-nm to hundreds of  $\mu\text{m}$  made by a combination of MEMS processes and subsequent FIB milling. The main issues addressed in this paper are: (i) large area patterning up to full-wafer size area and (ii) multiple length-scale apertures ranging from 100 nm to several 100s  $\mu\text{m}$ . The shadow mask deposition method has a high flexibility in choice of source materials and target surfaces, e.g. bio/chemically active layer, suspended MEMS/NEMS. The new type of shadow mask allows for combined micro- and nanostructures to be made side-by-side in a single evaporation step. It furthermore allows cost-efficient replication on large-area scale because the shadow mask can be reused. The presented results confirm the large application area for the shadow mask method as a general purpose patterning method beyond lithography

#### Acknowledgements

The authors thank CMI staff for fruitful discussions about micro fabrication and EMPA staff for FIB milling. This study was financially supported by EPFL and TOP NANO 21.

#### References

- [1] A. Kumar, G.M. Whitesides, *Appl. Phys. Lett.* 63 (1993) 2002–2004.
- [2] B. Michel, A. Bernard, A. Bietsch, E. Delamarque, M. Geissler, D. Juncker, H. Kind, J.-P. Renault, H. Rothuizen, H. Schmid, P. Schmidt-Winkel, R. Stutz, H. Wolf, *IBM J. Res. Dev.* 4 (5) (2001) 697–719.
- [3] S.Y. Chou, P.R. Krauss, P.J. Renstrom, *J. Vac. Sci. Technol. B* 14 (1996) 4129–4133.
- [4] K. Wilder, C.F. Quate, D. Adderton, R. Bernstein, V. Elings, *Appl. Phys. Lett.* 68 (1998) 2527–2529.
- [5] G.J. Burger, E.J.T. Smulders, J.W. Berenschot, T.S.J. Lammerink, J.H.J. Fluitman, S. Imai, *Sensors Actuators A* 54 (1996) 669–673.
- [6] J. Brugger, C. Andreoli, M. Despont, U. Drechsler, H. Rothuizen, P. Vettiger, *Sensors Actuators* 76 (1999) 329–334.
- [7] A. Tixier, Y. Mita, J.P. Gouy, H. Fujita, *J. Micromech. Microeng.* 10 (2000) 157–162.
- [8] R.J. Jackman, D.C. Duffy, O. Cherniavskaya, G.M. Whitesides, *Langmuir* 15 (1999) 2973–2984.
- [9] G.M. Kim, B. Kim, J. Brugger, in: *Proceedings of the 11th International Conference on Solid-State Sensors and Actuators*, 2001, pp. 1632–1635, Submitted to *Sensors and Actuators*.
- [10] M. Deshmukh, D.C. Ralph, M. Thomas, J. Silcox, *Appl. Phys. Lett.* 75 (1999) 1631–1633.
- [11] J. Brugger, J.W. Berenschot, S. Kuiper, W. Nijdam, B. Otter, M. Elwenspoek, *Microelectron. Eng.* 53 (2000) 403–405.
- [12] M. Koelbel, R.W. Tjerkstra, J. Brugger, C.J.M. van Rijn, W. Nijdam, J. Huskens, D.N. Reinhoudt, *NanoLetters* (2002) in press.